Journal of Pharmaceutical and Applied Chemistry

ISSN: 2357-0210 VOLUME 3, ISSUES 1, 2017 www.egyptfuture.org/ojs/

Design, Synthesis and QSAR Studies of Novel 1,3,4-Triarylpyrazoles as Anti-breast Cancer Agents

Amel M. Farrag, Marwa F. Harras and Magda M.F. Ismail*

Department of Pharmaceutical Chemistry, Faculty of Pharmacy (Girls), Al-Azhar University, Cairo, Egypt

Received: 5 Jun. 2016, Revised: 22 Oct. 2016, Accepted: 25 Oct. 2016.
Published online: 1 Jan. 2017.

Abstract:A series of fourteen novel 1,3,4-triarylpyrazoles were synthesized and evaluated for their antiproliferative activity against human breast cancer MCF7 cell line. Cells were exposed to different concentrations of compounds (0.1, 10, 100, 1000 µM) for 72 hours. Then the viability of treated cells was determined using MTT technique. Compound **7a** was found to exhibit significant antiproliferative activity (IC_{50} = 6.95 µM). Using flow cytometric analysis, compound **7a** was observed to induce apoptosis and to block the cell cycle at G2/M phases in MCF7 cells. 3D-Pharmacophore modeling and quantitative structure-activity relationship (QSAR) analysis were combined to explore the structural requirements controlling the observed anti-tumor properties.

Keywords: Pyrazole; Synthesis; MCF7 breast cancer cell line; cell cycle profile; apoptosis; 3D pharmacophore; QSAR study.

1 Introduction

Breast cancer is the most common type of female cancer [1]. It is a leading cause of morbidity and mortality worldwide with over a million cases yearly [2]. Despite advances in the early detection of breast cancer and the advent of novel targeted therapies, breast cancer still remains a significant public health problem [3]. In addition, efficacy of chemotherapy has not been substantially increased and undesirable side effects are still unacceptably high. Therefore, the search for novel chemotherapeutic agents for more effective cancer treatments is urgently required. [4].

On the other hand, pyrazoles constitute an important heterocyclic family that has been found to possess significant antitumor activity with excellent IC_{50} (concentration required for 50% inhibition of cell growth) [5]. For example, the two pyrazole derivatives in the market, Ruxolitinib (Jakavi®, Novartis) [βR-cyclopentyl-4-(7*H*-pyrrolo[2,3-d]pyrimidin-4-yl)-1*H*-pyrazole-1-propanenitrile] [6] and Crizotinib (XALKORI®) [3-[(1R)-1-(2,6-Dichloro-3-fluorophenyl)ethoxy]-5-[1-(4-piperidinyl)-1H-pyrazol-4-yl]-2-pyridinamine] [7].

Although the skeleton of pyrazole plays an important role in its biological effects, the type of peripheral substituents is also crucial [8]. Among the reported studies, 1,3-diarylpyrazole derivative, ethyl 4-(3-(4-chlorophenyl)-1-phenyl-1H-pyrazol-4-yl)-6-methyl-2-thioxo-1,2,3,4-tetrahydropyrimidine-5-carboxylate bearing dihydropyrimidine at C-4 of the pyrazole ring showed excellent growth inhibition of MCF-7 cell lines with 70.6% and 99.2%, at 10 µM and 100 µM concentrations, respectively [9]. Moreover, 3-methyl-4,5-dihydronaphtho[1,2-c]pyrazol-2-yl analog [10] andthe N'-(1-{1-[4-nitrophenyl]-3-phenyl-1*H*-pyrazol-4-yl}methylene)-2-chlorobenzohydrazide displayed significant activity against MCF7 cell line [11].

Interestingly, Huang *et al.* reported a novel class of potent inhibitors of CDK2/cyclin E based on N-((1,3-diphenyl- 1H-pyrazol-4-yl)methyl)aniline scaffold. N-((3-(4-chlorophenyl)-1-phenyl-1H-pyrazol-4-yl)methyl)-4-fluoroaniline displayed the most potent inhibition activity which inhibited the growth of MCF7 and B16-F10 cell lines with IC_{50} values of 1.88 and 2.12 µM and inhibited the CDK2/ cyclin E holoenzyme activities with IC_{50} of 0.98 µM [12]. In addition,2- [(3-(4-methoxyphenyl)-1-phenyl-1*H*-pyrazol-4-yl)methylene]-1*H*-indene-1,3(2*H*)-dione showed high anti-breast cancer activity with IC_{50} value of 3.9 µM against MCF7 (human breast adenocarcinoma) cell line [13].

In view of the facts mentioned above, most of the reported studies were concerned with substitution at C-4 position of the pyrazole ring which has inspired our study to design a series of new 1,3,4-triaryl pyrazole derivatives bearing different aryl moieties at C-4 positions either attached

directly or via methine linker. The latter designed compounds were synthesized to evaluate the anticancer activity of new compounds against breast cancer MCF7 cell line. For the most active compound, the effect on the normal cell cycle profile and induction of apoptosis were performed in the MCF7 cell line in order to investigate its mechanism of action. In this work, quantitative structure-activity relationship (QSAR) studies will be performed, not only for validating the observed pharmacological properties but also, for investigating the most important parameters controlling these properties.

2 Results and Discussion

2.1 Chemistry

The target compounds were synthesized according to the steps outlined in **Schemes 1** and **2**. The key intermediates 1-(1-(4-substitutedphenyl)ethylidene)-2-phenylhydrazine **2a,b** were synthesized by condensation of the synthesized 4-benzyloxyacetophenone or 4-aminoacetophenone and phenylhydrazine. Treatment of the hydrazone derivatives **2a** with Vilsmeier-Haack reagent (DMF-$POCl_3$) in three equivalents [14] led to corresponding 4-formylpyrazole derivatives **3a.**

In case of the amino hydrazone **2b,** on Vilsmeier-Haack formylation [14] afforded 4-formyl-pyrazolyl-dimethylformimidamide **3b**. ^{1}H NMR spectrum of **3b** showed two singlets at 3.29 and 3.34 ppm corresponding to the N,N-dimethyl groups. Compounds **3a,b** were allowed to react with malononitrile in ethanol containing few drops of piperidine [15] to afford the arylidene malononitrile derivatives **4a,b**. It is believed that malononitrile adds to the N,N-dimethylformimidamide derivative **3b** to yield **4b.** IRspectrum of **4b** showed strong band at 2221 cm^{-1} corresponding to 4 cyano groups, its ^{1}H NMR spectrum showed the disappearance of the dimethylamino signals of **3b** in addition to the appearance of two doublets at 6.69 and 7.35 ppm for the dicyanoethylidene protons.

Cycloaddition of hydrazine hydrate or phenyl hydrazine on **4a,b** in the presence of piperidine drops [16] furnished pyrazole and pyrazoline derivatives **5a,b** and **6a,b** respectively. The structure assignment of the products was established by microanalytical and spectral data. IR spectrum of **5a** showed absorption bands at 3388, 3367 and 3282 cm^{-1} assigned to two NH_2 groups with the observed lack of the two cyano groups' bands. Its ^{1}H NMR spectrum revealed one singlet at 4.25 ppm representing four protons of two NH_2 groups exchangeable with D_2O.

In addition, the arylidene malononitriles **4a,b** were reacted with cyclohexanone in presence of ammonium acetate [17] to give tetrahydroquinoline derivatives **7a,b**. ^{1}H NMR spectrum of **7a** showed two multiplets at the range 1.67-1.83 and 2.65-2.70 ppm corresponding to aliphatic protons of cyclohexane moiety, another singlet appeared at 6.57 ppm which is attributed to the exchangeable NH_2 protons. In addition, ^{13}C NMR spectrum of **7a** revealed three peaks in the aliphatic region at 22.25, 24.94 and 25.56 ppm for the cyclohexane carbons. (Scheme 1)

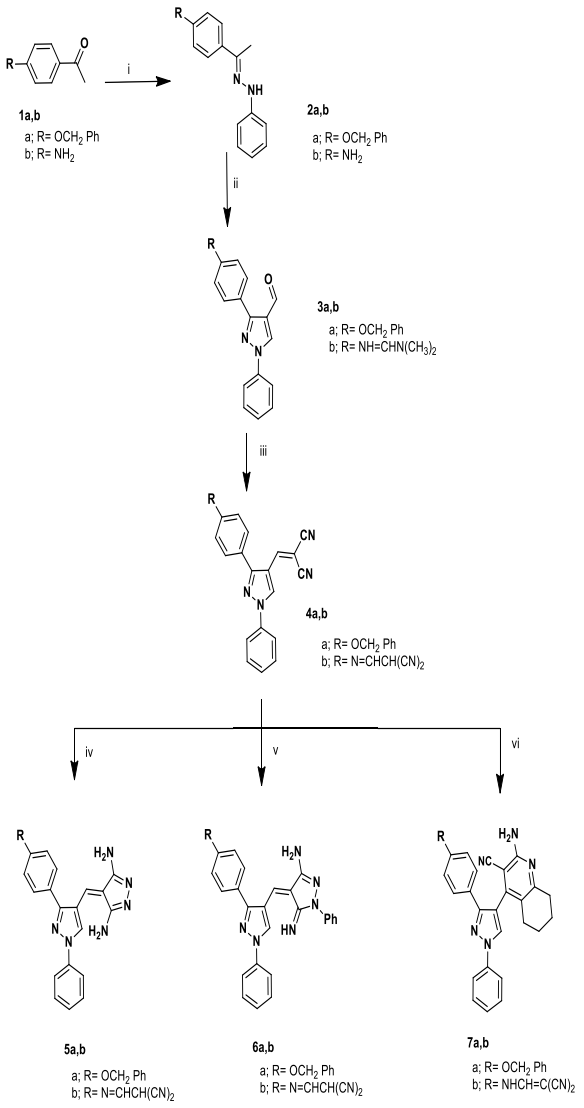

Scheme1

Reagents and condition: (i) Phenylhydrazine, EtOH, glacial acetic, r.t.(ii) $POCl_3$, DMF, reflux. (iii) malononitrile, EtOH, piperidine, reflux. (iv) hydrazine hydrate, EtOH, piperidine, reflux. (v) phenylhydrazine, EtOH, piperidine, reflux.(vi) cyclohexanone, EtOH, ammonium acetate, reflux.

As shown in Scheme 2, Compound **3a** was allowed to react with semicarbazide hydrochloride in presence of sodium acetate to form **8a** or with thiosemicarbazide in the presence of acetic acid [18] to form **8b**. IR spectrum of **8a** showed absorption bands at 3222 and 3150 cm^{-1} corresponding to two NH groups. The ^{1}H NMR spectrum of **8a** (DMSO-d_6, δ ppm) showed two singlets at 6.39 and 10.03 corresponding to two NH protons exchangeable with D_2O, its ^{13}C NMR spectrum displayed peaks at 150.44 and 158.49 ppm for the triazolyl and the carbonyl carbons, respectively. On the other hand, Cyclocondensation of the aldehyde **3a** with urea or thiourea and ethylcyanoacetate in the presence of sodium ethoxide [19] gave the

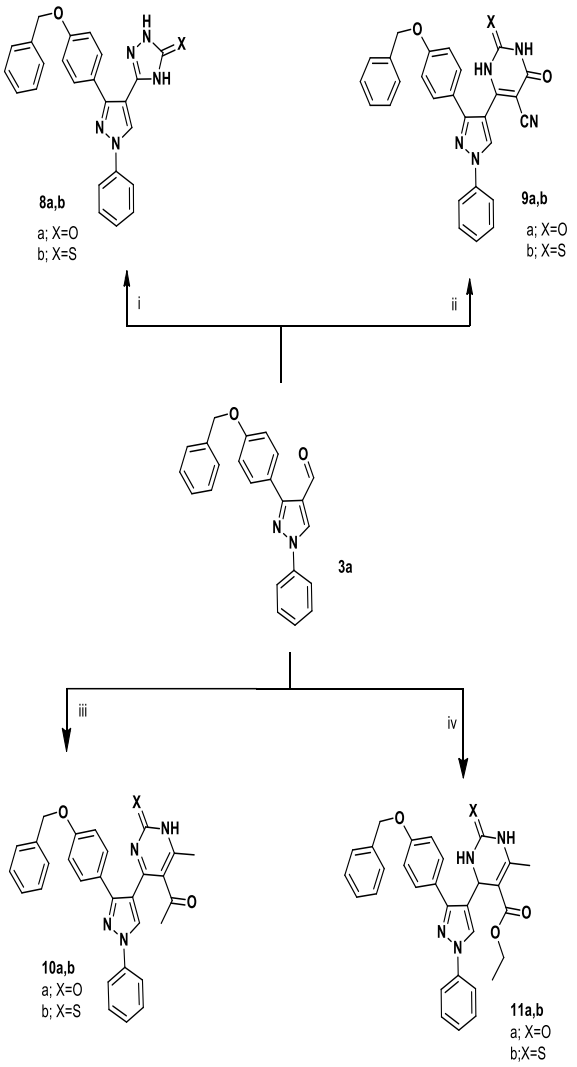

Scheme 2

Reagents and condition: (i) semi/thiosemicarbazide, EtOH, sodium acetate/ glacial actic acid, reflux. (ii) urea/thiourea, ethylcyanoacetate,sodium ethoxide, reflux. (iii) urea/thiourea, acetylacetone, ethanol, HCl reflux. (iv) urea/thiourea, ethylacetoacetate, ethanol, HCl reflux.

corresponding 2-oxo (thioxo) pyrimidine derivatives **9a,b**. IR spectrum (KBr, cm^{-1}) of compound **9a** showed strong absorption band at 3347 cm^{-1}, assigned to the two NH groups, at 2221 cm^{-1} for C≡N group and at 1692 and 1637 cm^{-1} corresponding to the two carbonyl amide groups. Furthermore, an acid-catalyzed three components condensation reaction[20] in which a mixture of 1,3-dicarbonyl compounds (acetylacetone or ethylacetoacetate), the aldehydic compound **3a** and urea or thiourea, in absolute ethanol and few drops of concentrated hydrochloric acid was refluxed to afford Biginelli compounds. It was a convenient route to achieve the preparation of the desired heterocyclic compounds **10a,b** and **11a,b**. IR spectrum of **11a** showed strong absorption bands at 3341 and 3145 cm^{-1} assigned to the two NH groups and at 1701, 1655 cm^{-1} comprising the two carbonyl groups. Its ^1H NMR spectrum revealed signals at 1.04 ppm as a triplet corresponding to the protons of OCH_2-$C\underline{H_3}$moiety, at 2.27 ppm as a singlet for the protons of $C\underline{H_3}$, at 3.42 ppm as a quartet corresponding to the protons of $OC\underline{H_2}$-CH_3 moieties, at 5.38 ppm as singlet for CH of pyrimidine and at 9.30 and 9.98 ppm attributed to the two exchangeable NH protons.

2.2 Anti-tumor properties

The *in-vitro* anti-tumour activity against human breast cancer cells (MCF7) of the 14 test compounds was achieved in the cell culture lab, college of pharmacy, Al-Azhar University, Cairo, Egypt. Doxorubicin was used as a reference standard and showed IC_{50} 2.008 μM.

The anticancer MCF7 profile suggested that, test compounds showed variable activity compared to reference drug as shown in Table1. 3,5-diamino-pyrazole derivatives **5a,b**. It is noticed that compound **5b** carrying [$(CN)_2CH$-CH=N-] (IC_{50}=8.71 μM) displayed 1.7 folds the activity of its analog which bears $PhCH_2O$ (**5a**) (IC_{50}=15.13 μM). On the contrary in compounds **6** and **7,** it was observed that the analogs bearing $PhCH_2O$ (**6a** and **7a**) displayed enhanced anti-proliferative activities (IC_{50}'s= 36.3 and 6.95 μM respectively) than their counterparts **6b** and **7b** (c.f. scheme 1).

Table 1 IC_{50} of the tested compounds against human breast cancer cells MCF7.

Entry	Compound	IC_{50} (μM)
1	**5a**	15.13
2	**5b**	8.71
3	**6a**	36.3
4	**6b**	295.12
5	**7a**	6.95
6	**7b**	301.99
7	**8a**	12.6
8	**8b**	1050
9	**9a**	54.95
10	**9b**	75.80
11	**10a**	1300
12	**10b**	1100
13	**11a**	1050
14	**11b**	154.88
15	**Doxorubicin**	2.008

In scheme 2, reaction of starting compound **3a** with semicarbazide/ thiosemicarbazide yielded the corresponding 1,2,4-triazolin-3-one **8a** or 1,2,4-triazolin-3-thione **8b** with IC_{50}'s= 12.6 and 1050 μM respectively. The abolished anti-breast carcinoma activity may be attributed to the presence of lipophilic nature of S in **8b** instead of O in **8a**. Moreover, reaction of pyrazol-4-carboxaldehyde with urea or thiourea and ethylcyanoacetate produced pyrimidine-2,4-dione-5-carbonitrile **9a** or pyrimidine-4-one-2-thione-5-carbonitrile **9b** which exhibited moderate activity (IC_{50}'s=54.95 and 75.8 μM) respectively. Lower anti-proliferative activities against MCF7 were observed for 5-acetylpyrimidin-2-one(thione) **10a,b** and pyrimidin-2-one(thione)-5-carboxylates **11a,b**.

2.2.1 Effects of the 7a on the morphology of MCF7

cells

The most active compound **7a** was examined to determine whether the decrease in cell viability/ number was caused by apoptosis. Cells were treated with the IC_{50} of **7a** for 24hrs, then cells were stained with the nuclear stain for 30 min and the images were viewed with an epifluorescence microscope.

In treatment with the pre-calculated Ic_{50} of **7a,** we observed a reduction of the cell density and proliferation in addition to an apparent morphological change, such as, chromatin condensation, destructive fragmentation of the nuclear material and loss of DNA integrity as indication of apoptosis (figure 1) which was in parallel with their cell cycle analysis.

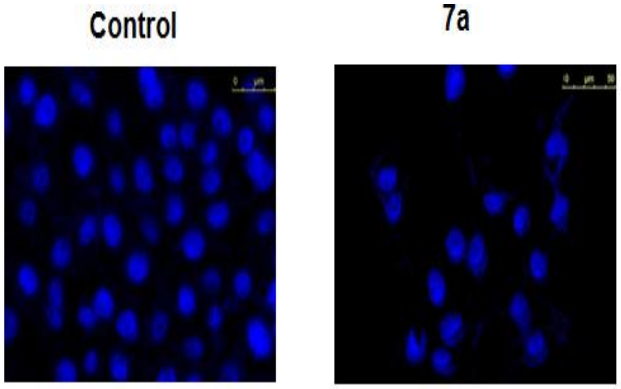

Figure 1 Effects of **7a** on cell morphology and cellular viability

2.2.2 Cell cycle analysis and detection of apoptosis

The most active compound **7a** was selected to be further studied regarding to its effects on cell cycle progression and induction of apoptosis in the MCF7 cell line. The MCF7 cells were incubated with GI_{50} concentration of **7a** for 24 h and its effect on the normal cell cycle profile and induction of apoptosis was analyzed. Exposure of MCF7 cells to **7a** resulted in an interference with the normal cell cycle distribution of this cell line.

Compound **7a** induced a significant increase in the percentage of cells at pre-G1 and G2/M phases by 17.1 and 3.4 folds respectively, compared to control. Such increase was accompanied by a disappearance of cells at the S phase of the cell cycle. Accumulation of cells in pre-G1 phase which was confirmed by the presence of a sub-G1 peak in the cell cycle profile analysis may result from degradation or fragmentation of the genetic materials indicating a possible role of apoptosis in compound **7a**-induced cancer cell death and cytotoxicity. While the accumulation of the cells in G2/M phases may result from G2/M arrest (Figures 2 and 3).

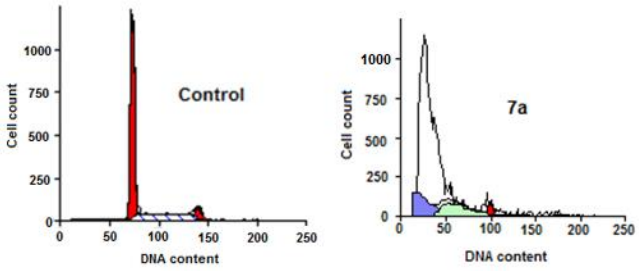

Figure 2 Effect of **8b** on DNA-ploidy flow cytometric analysis of MCF7 cells. The cells were treated with **8b** (2.11 μM), for 24 h, and the harvested cells were subjected to Cell-cycle analysis using a FACS Calibur flow cytometer.

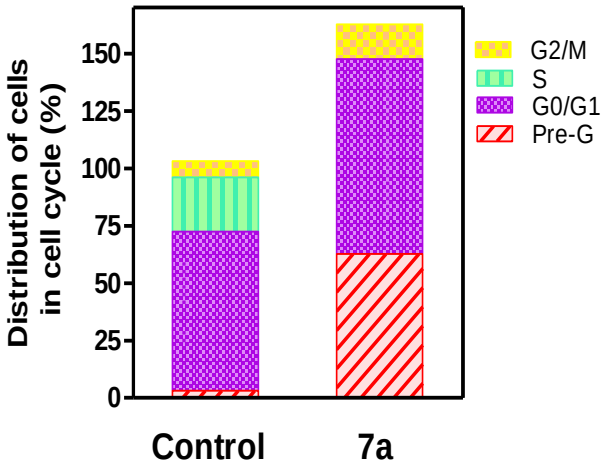

Figure 3 Bar chart shows percentage of MCF7 cells at each phase of cell cycle in control cells and cells treated with compound **8b**.

2.3 QSAR study

2.3.1 3D-QSAR pharmacophore modeling

This study was performed using Discovery Studio 2.5 software (Accelrys Inc., San Diego, CA, USA), which permits pharmacophore generation; structural alignment; activity prediction and 3D database creation [21-22]. 3D-QSAR pharmacophore protocol (Catalyst HypoGen algorithm) was used to derive structure activity relationship hypothesis models from a set of ligands with known activity values on a given biological target. The training set is composed of fourteen synthesized compounds from the present study with measured IC_{50} against MCF7 cancer cell line. The pharmacophore features used are hydrogen bond acceptor (HBA), hydrogen bond donor (HBD), hydrophobic (HYP), and ring aromatic (RA). Fisher validation was applied and set to 95% significance. Pharmacophores were then generated in HypoGen module and the top ten scoring hypotheses were exported. HypoGen identifies features common to the active compounds and excludes features common to the inactive compounds within conformational allowable regions of space. It further estimates the activity

of our new synthesized and tested compounds using regression parameters. The parameters were computed by regression analysis using the relationship of geometric fit value versus the activity. The better the geometric fit, the greater is the activity prediction of the compound.

2.3.2 3D-QSAR pharmacophore study results

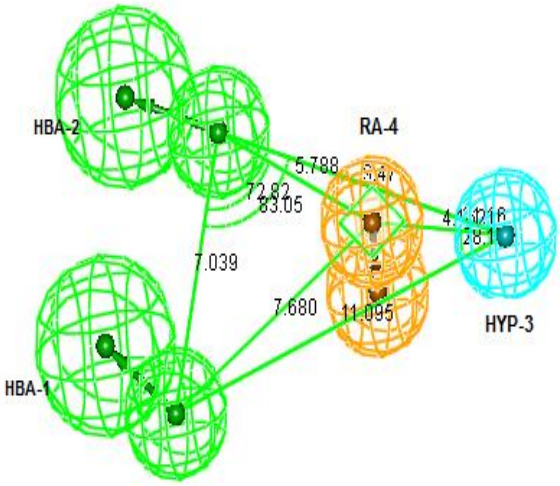

Figure 4 Constraint distances and angles between features of the generated top pharmacophore model with the features considered hydrogen bond acceptor (HBA) colored in green, ring aromatic (RA) colored in orange, hydrophobic (HYP) colored in cyan.

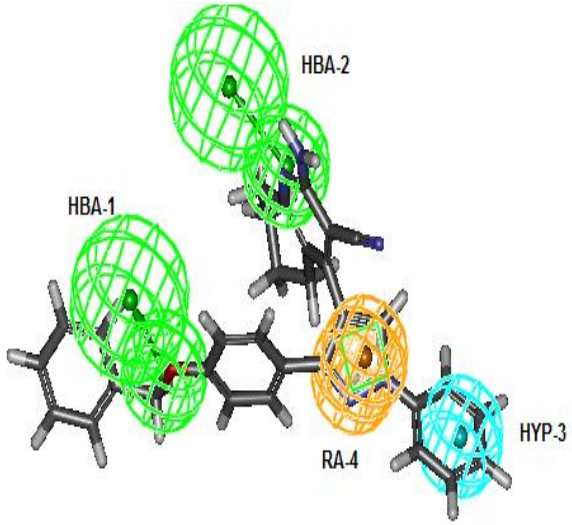

Figure 5 Compound **7a** fitted in the pharmacophore with fit value12.04.

Ten predictive pharmacophore models (hypothesis) were generated via aligning different conformations of the represented training set ligands to bind with the generated pharmacophore models. These pharmacophore models were exported for further studies. The top pharmacophore model generated, Hypothesis 1, was developed having two HBA, one HYP, and one RA feature as shown in (figure. 4) with constraint distances and angles between its features as described in Table 2. In (figure 5) **7a** are represented with the best generate pharmacophore model. It has highest fit value of 12.04 and highest cytotoxic activity against Human Breast MCF7 Cancer cell line with IC_{50} of 6.95 µM. Four pharmacophore features were considered, where O of benzyloxy group fits with (HBA-1), N of tetrahydroquinoline moiety fits with (HBA-2), phenyl ring of the N-phenypyrazole fits with (HYP-3) and additionally the pyrazole ring fits with (RA-4).

Table 2 Constraint distances (Å) and angles (^{0}) between features of the generated pharmacophore.

Constraint distances (Å)	Constraint angles (^{0})
(HBA-1) - (HBA-2), 7.039;	(HBA-1) - (HBA-2) – (HYP-3), 53.05;
(HBA-1) - (HYP-3), 11.095;	(HBA-1) - (HBA-2) – (RA-4), 72.82;
(HBA-1) - (RA-4), 7.680;	(HBA-1) - (HYP-3) – (RA-4), 28.14;
(HBA-2) – (HYP-3), 9.471;	(HBA-2) - (HYP-3) – (RA-4), 21.16.
(HBA-2) – (RA-4), 5.788;	
(HYP-3) – (RA-4), 4.162	

2.3.3 Validation of 3D-QSAR pharmacophore

The pharmacophore models generated should be statistically significant, able to predict the activities of new chemical compounds and retrieve active compounds from the database. The selection of the generated pharmacophore model (hypothesis 1) was based on its validation using three methods; cost analysis, activity prediction and Fisher validation test.

HypoGen selects the best hypothesis by applying a cost analysis. A larger difference between the fixed and null costs than that between the fixed and total costs of each hypothesis signifies the quality of a pharmacophore model. The significance of the hypothesis also depends on the cost difference which is measured between the null cost and the total cost of a given hypothesis. The larger the value of the cost difference, the more statistically significant the hypothesis is believed to be. In detail, the null cost and fixed cost of the ten pharmacophore hypothesis were equal to 174.58 and 51.46, respectively. Hypothesis 1 is the best generated pharmacophore hypothesis as it is characterized by the lowest total cost (78.90), the highest cost difference between null and total hypothesis cost (95.68), and the best correlation coefficient (0.94) which indicates the capability of the pharmacophore model to predict the activity of the training set compounds.

The pharmacophore model (hypothesis 1) was also validated through activity prediction of the synthesized structures as training set. The predicted activities of the training set through the pharmacophore model as well as their fit values are represented in Table.3.

Table 3 Fit values and estimated activities for the synthesized compounds mapped with the generated 3D-

pharmacophore model.

Entry	Compound	Estimated activity	Observed activity	Fit value
1	**5a**	26.2	15.13	11.626
2	**5b**	16.44	8.71	11.828
3	**6a**	21.86	36.3	11.704
4	**6b**	113.76	295.12	10.988
5	**7a**	9.87	6.95	12.049
6	**7b**	722.40	301.99	9.663
7	**8a**	29.65	12.6	11.572
8	**8b**	479.00	1050	10.364
9	**9a**	99.42	54.95	11.046
10	**9b**	66.56	75.80	11.221
11	**10a**	400.79	1300	10.441
12	**10b**	655.17	1100	10.227
13	**11a**	600.173	1050	10.266
14	**11b**	112.35	154.88	10.993

Fischer validation is another approach for pharmacophore model validation. The Fischer validation confidence level for hypothesis 1 is 95%. This validation method checks the correlation between the chemical structures and biological activity. This method generates pharmacophore hypothesis using the same parameters as those used to develop the original pharmacophore hypothesis by randomizing the activity data of the training set compounds.

2.3.4 QSAR modeling

Despite of the significance of pharmacophoric hypotheses for understanding ligand molecule affinity and 3D search queries, their predictive value as 3D-QSAR models is generally limited by steric shielding and bioactivity-modulating auxiliary groups (electron-donating or withdrawing functionalities) [23-25]. Thus, a classical QSAR analysis was employed to search for the best combination of orthogonal pharmacophores using a fit value and other structural descriptors (connectivity, topological, etc.) capable of explaining bioactivity variation across a collected list of the descriptors, allowing different pharmacophoric models competing within the 3D-QSAR framework. A set of 14 newly synthesized pyrazole derivatives was used as training set with their measured pIC_{50} (the negative logarithmic value of the concentration required to produce 50% inhibition of the cancer cells) against MCF7 cancer cell line for the present QSAR modeling. Many molecular descriptors were calculated for each compound employing a calculated molecular properties module. 2D Descriptors involved: AlogP, fingerprints, molecular properties, surface area, volume and topological descriptors, and the 3D descriptors: dipole, jurs descriptors, principle moments of inertia and shadow indices. Furthermore, the training set compounds were fitted (using the best-fit option) against representative pharmacophores and their fit values were added as additional descriptors. Moreover, energies of highest occupied and lowest unoccupied molecular orbitals (HOMO and LUMO) [26] of each of the training set compounds were determined using this software and imported as additional descriptors. Multiple linear regression (MLR) protocol were employed to search for optimal QSAR models that combine high quality binding pharmacophores with other molecular descriptors and being capable of correlating bioactivity variation across the used training set collection. QSAR models were validated employing leave one-out cross-validation, r^2 (squared correlation coefficient value) and r^2 prediction (predictive squared correlation coefficient value) [26]. Statistical outliers were identified from experimental versus predicted plots.

2.3.5 QSAR study results

Equation 1 represents the best performing QSAR model;

$-logIC_{50}$ = -0.307 + 1.565 **[ALogP]** - 8.369e-002 **[Molecular_Fractional Polar SurfaceArea]** + 1.207 **[Fit value]**

According to Equation 1, QSAR model was represented graphically by scattering plots of the experimental versus the predicted bioactivity values $-logIC_{50}$ for the training set compounds as shown in (Figure 6). The method used to build the model was Least-Squares, r^2 = 1, r^2 (adj) 1, r^2 (pred) 1, Least-Squared error 0, where r^2 (adj) is r^2 adjusted for the number of terms in the model; r^2 (pred) is the prediction r^2, equivalent to q^2 from a leave-1-out crossvalidation.

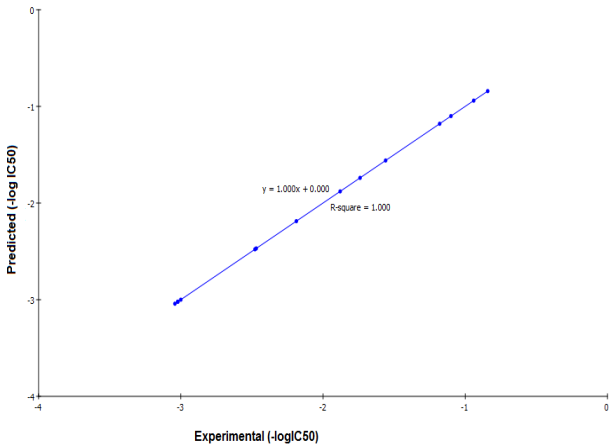

Figure 6 Predicted versus experimental IC_{50} of the tested compounds against MCF7 (breast) human tumor cell line.

In conclusion, Equation 1 describes that the anti-proliferative activity of the synthesized compounds against the breast MCF7 cancer cell line is affected by two molecular descriptors AlogP and molecular fractional polar Surface. It was found that the anti-proliferative activity is positively correlated with the increase in the hydrophobicity (ALogP) and the decrease in the molecular fractional polar surface area of the synthesized compounds.

2.3.6 Validation of QSAR

QSAR models were validated employing leave one-out cross-validation where r^2 (squared correlation coefficient

value) which is 1, r^2 (pred) is the prediction r^2, equivalent to q^2 from a leave-1-out cross-validation which is 1.

Table 4 Estimated activity data of the training set against MCF7 (breast cancer) cell line andcalculated descriptors governing activity according to Equation 1.

Entry	Compound	Experimental activity (-log IC_{50})	Predicted activity (-log IC_{50})	Residual
1	**5a**	-1.1798	-1.1798	1.02783e-09
2	**5b**	-0.9400	-0.9405	-7.05977e-10
3	**6a**	-1.5599	-1.5599	1.52984e-11
4	**6b**	-2.4700	-2.4698	-2.06975e-10
5	**7a**	-0.8419	-0.8419	-6.89453e-10
6	**7b**	-2.4799	-2.4785	8.45648e-10
7	**8a**	-1.1003	-1.1003	-3.22342e-09
8	**8b**	-3.0211	-3.0211	3.27683e-09
9	**9a**	-1.7399	-1.7395	1.45207e-08
10	**9b**	-1.8796	-1.8796	-1.42041e-08
11	**10a**	-3.1139	-3.1139	3.62979e-10
12	**10b**	-3.0413	-3.0413	-9.38243e-10
13	**11a**	-3.0211	-3.0211	-1.11402e-08
14	**11b**	-2.1900	-2.1875	1.10279e-08

Validation was also employed by measuring the residuals between the experimental activity and the predicted activity of the training set. The observed activities and those provided by QSAR studies were presented in Table 4. It should be noted that the predicated antitumor activities by our QSAR models were very close to those experimentally observed, indicating that these models can be safely applied for predication of more effective hits having the same skeletal framework as that of the potent antitumor compound.

3. Conclusion

In the process of anti-cancer drug discovery, to find new potential anti-breast cancer agents, we synthesized a novel series of pyrazole derivatives. Cytotoxicity evaluation against MCF7 cell line revealed that, tetrahydroquinoline derivative **7a** was the most potent anticancer one and. Further biological assessment of **7a** using flow-cytometric analysis, revealed that it induced cell cycle arrest at G2/M phase and also, showed accumulation of cells in pre-G1 phase which indicates a possible role of apoptosis. 3D-QSAR pharmacophore modeling afforded an HYPOGEN with four chemical features: 2 HBA, 1 HYP and 1 RA. QSAR studies showed good predictive and statistically significant descriptor model with r^2 1. The most important descriptors in the QSAR equation were ALogP, molecular_FPSA and fit value derived from mapping of the synthesized compounds into the generated pharmacophore. The combination of 3D-pharmacophore modeling and QSAR provides as an effective technique for understanding the observed pharmacological properties and thus could be adopted for developing effective lead structures.

4 Experimental

All chemicals were purchased from VWR International Merck, Germany or Sigma-Aldrich and used without further purification. Melting Points were carried out by open capillary tube method using Stuart SMP3 Melting Point apparatus and they are uncorrected. Elemental Microanalysis was carried out at the Regional Center for Mycology and Biotechnology, Al-Azhar University. Infrared spectra were recorded using potassium bromide discs on Bruker ATR/FTIR Spectrophotometer at the Armed Forces Laboratories. ^{1}H NMR and ^{13}C NMR Spectra were recorded on a Varian Gemini 300 MHz Spectrophotometer, the spectra were run at 300 MHz in deuterated dimethylsulfoxide (DMSO-d_6) at the Armed Forces Laboratories. Chemical shifts were expressed in δ units and were related to that of the solvents. As for the proton magnetic resonance, D_2O was carried out for NH and OH exchangeable protons. Mass Spectra were recorded using Shimadzu Gas Chromatograph Mass spectrometer-Qp 2010 plus (Japan) at the Regional Center for Mycology and Biotechnology, Al-Azhar University. All the reactions were followed by thin layer chromatography using silica gel F254 plates (Merck) and were visualized by UV-lamp. Compounds **1** and **2b** were prepared according to reported procedures [27, 28]

4.1. Synthesis

4.1.1. Synthesis of 1-(1-(4-(benzyloxy)phenyl) ethylidene)-2-phenylhydrazine 2a

A mixture of phenylhydrazine (1.08 g, 0.01 mole) in glacial acetic acid (1 mL) was added to a solution of 4-benzyloxy acetophenone (2.26 g, 0.01 mol) in ethanol (30 mL). Then, the reaction mixture was stirred at room temperature for 24 h, concentrated under reduced pressure and poured onto ice/water. The solid formed was collected, washed with water, dried and recrystallized from ethanol.

Yield 65%; m.p. 132-135 ^{o}C; IR (KBr, cm^{-1}): 3352 (NH), 3030 (CH aromatic), 2925 (CH aliphatic), 1599 (C=N &C=C); ^{1}H NMR (DMSO-d_6) δ (ppm): 2.46 (s, 3H, CH_3), 5.20 (s, 2H, OCH_2), 7.09 (d, 2H, aromatic H, J = 9 Hz), 7.33-7.47 (m, 10H, aromatic H), 7.91 (d, 2H, aromatic H, J = 9 Hz), 10.31 (s, 1H, NH; exchangeable with D_2O); MS, m/z: 316 (M^+, 100%); Anal. Calcd. For $C_{21}H_{20}N_2O$ (316.16): C, 79.72; H, 6.37; N, 8.85, Found: C, 79.98; H, 6.46; N, 8.98.

4.1.2. General procedure for the synthesis of compounds 3a,b

A mixture of DMF (2.55 g, 0.035 mol) and $POCl_3$ (5.40 g, 0.035 mol) was cooled at 0ºC before being stirred at that temperature. A solution of **2a,b** (0.012 mol) in DMF (3 mL) was added drop wise to the Vilsmeiere-Haack reagent, warmed to room temperature, and heated at 70-80 ºC for 5 h. After cooling to room temperature, the mixture was basified with cold saturated K_2CO_3 solution. The precipitate was filtered, washed with water and crystallized from ethanol.

3-(4-(benzyloxy)phenyl)-1-phenyl-1*H*-pyrazole-4-carbaldehyde **3a**

Yield 87%; m.p. 140-142 ºC; IR (KBr, cm^{-1}): 3029 (CH aromatic), 2911 (CH aliphatic), 1669 (C=O), 1605 (C=N &C=C); ^{1}H NMR (DMSO-d_6) δ (ppm): 5.18 (s, 2H, OCH_2), 7.13 (d, 2H, aromatic H, *J* = 9 Hz), 7.38-7.59 (m, 8H, aromatic H), 7.89 (d, 2H, aromatic H, *J* = 9 Hz), 7.96 (d, 2H, aromatic H), 9.29 (s, 1H, CH of pyrazole), 9.96 (s, 1H, CHO); MS, m/z: 354 (M^+, 1.31%); Anal. Calcd. For $C_{23}H_{18}N_2O_2$ (354.14): C, 77.95; H, 5.12; N, 7.90, Found: C, 78.12.; H, 5.17; N, 7.98.

N'-(4-(4-formyl-1-phenyl-1*H*-pyrazol-3-yl)phenyl)-N,N-dimethylformimidamide **3b**

Yield 61%; m.p. 231-233 ºC; IR (KBr, cm^{-1}): 3055 (CH aromatic), 2938 (CH aliphatic), 1666 (C=O), 1603 (C=N &C=C); ^{1}H NMR (DMSO-d_6) δ (ppm): 3.29 (s, 3H, N-CH_3), 3.34 (s, 3H, N-CH_3), 7.41-7.68 (m, 5H, aromatic H), 7.89 (d, 2H, aromatic H, *J* = 7.8 Hz), 7.97 (d, 2H, aromatic H, *J* = 7.8 Hz), 8.71 (s, 1H, N=CH), 9.34 (s, 1H, CH of pyrazole), 9.99 (s, 1H, CHO); MS, m/z: 318 (M^+, 100%); Anal. Calcd. For $C_{19}H_{18}N_4O$ (318.15): C, 71.68; H, 5.70; N, 17.60, Found: C, 71.89; H, 5.72; N, 17.89.

4.1.3. General procedure for the synthesis of compounds 4a,b

A mixture of compound **3a,b** (0.01 mol), malononitrile (1.32 g, 0.02 mol) and few drops of piperidine in ethanol (40 mL) was heated at 70ºC for 2h and then poured into water. The resulting solid formed was filtered off and crystallized from ethanol.

2-((3-(4-(benzyloxy)phenyl)-1-phenyl-1*H*-pyrazol-4-yl)methylene)malononitrile **4a**

Yield 74%; m.p. 130-132 ºC; IR (KBr, cm^{-1}): 3065 (CH aromatic), 2942 (CH aliphatic), 2193. 2160 (2 C≡N), 1611 (C=N &C=C); ^{1}H NMR (DMSO-d_6) δ (ppm): 5.12 (s, 2H, OCH_2), 7.07 (d, 2H, aromatic H, *J* = 9 Hz), 7.12-7.83 (m, 10H, aromatic H), 7.93 (d, 2H, aromatic H, *J* = 9 Hz), 8.43 (s, 1H, olefinic H), 8.84 (s, 1H, CH of pyrazole); MS, m/z: 402 (M^+, 0.74%); Anal. Calcd. For $C_{26}H_{18}N_4O$ (402.15): C, 77. 59; H, 4.51; N, 13.92, Found: C, 77.82.; H, 4.54; N, 14.13.

2-((3-(4-((2,2-dicyanoethylidene)amino)phenyl)-1-phenyl-1*H*-pyrazol-4-yl)methylene) malononitrile **4b**

Yield 83%; m.p. 308-310 ºC; IR (KBr, cm^{-1}): 3037 (CH aromatic), 2948 (CH aliphatic), 2221 (4 C≡N), 1610 (C=N), 1597 (C=C); ^{1}H NMR (DMSO-d_6) δ (ppm): 6.69 (d, 1H, $CH(CN)_2$, *J* = 8.4 Hz), 7.35 (d, 1H, N=CH, *J* = 8.4 Hz), 7.45-7.63 (m, 5H, aromatic H), 7.72 (d, 2H, aromatic H, *J* = 9 Hz), 7.92 (d, 2H, aromatic H, *J* = 9 Hz), 8.20 (s, 1H, olefinic H), 9.19 (s, 1H, CH of pyrazole); MS, m/z: 387 (M^+, 100%); Anal. Calcd. For $C_{23}H_{13}N_7$ (387.12): C, 71.31; H, 3.38; N, 25.31, Found: C, 71.42; H, 3. 36; N, 25.48.

4.1.4. General procedure for the synthesis of compounds 5a,b and 6a,b

A mixture of compounds **4a,b** (0.001 mol) and hydrazine hydrate or phenyl hydrazine (0.001 mol) in absolute ethanol (50 mL) containing catalytic amount of piperidine in was allowed to reflux for 8-12h. The resulting precipitate was filtered off and crystallized from ethanol.

4-((3-(4-(benzyloxy)phenyl)-1-phenyl-1*H*-pyrazol-4-yl)methylene)-4*H*-pyrazole-3,5-diamine (**5a**)

Yield 65%; m.p. 190-192 ºC; IR (KBr, cm^{-1}): 3388, 3367 &3282 (2 NH_2), 3035 (CH aromatic), 2924 (CH aliphatic), 1612 (C=N), 1597 (C=C); ^{1}H NMR (DMSO-d_6) δ (ppm): 4.25 (s, 4H, $2NH_2$; exchangeable with D_2O), 5.19 (s, 2H, OCH_2), 7.17 (d, 2H, aromatic H, *J* = 9 Hz), 7.34-7.71 (m, 10H, aromatic H), 7.99 (d, 2H, aromatic H, *J* = 9 Hz), 8.66 (s,1H, olefinic H), 9.10 (s, 1H, CH of pyrazole); ^{13}C NMR (DMSO-d_6) δ (ppm): 66.21, 111.68, 113.54, 113.66, 115.85, 118.05, 118.59, 118.85, 119.97, 124.79, 124.86, 126.00, 128.72, 128.90, 129.38, 131.85, 131.99, 139.01, 139.37, 148.81, 149.07, 149.42, 150.77, 153.68; MS, m/z: 434 (M^+, 0.96%); Anal. Calcd. For $C_{26}H_{22}N_6O$ (434.19): C, 71.87; H, 5.10; N, 19.34, Found: C, 72.03; H, 5.18; N, 19.51.

2-(((4-(4-((3,5-diamino-4*H*-pyrazol-4-ylidene)methyl)-1-phenyl-1*H*-pyrazol-3-yl)phenyl) imino)methyl)malononitrile **5b**

Yield 63%; m.p. 270-272 ºC; IR (KBr, cm^{-1}): 3344, 3217 &3121 (2 NH_2), 3055 (CH aromatic), 2924 (CH aliphatic), 2190 (2 C≡N), 1607 (C=N& C=C); ^{1}H NMR (DMSO-d_6) δ (ppm): 5.39 (s, 4H, $2NH_2$; exchangeable with D_2O), 6.68 (d, 1H, $CH(CN)_2$, *J* = 8.4 Hz), 7.33-8.00 (m, 10H, 9 aromatic H+ N=CH), 8.66 (s, 1H, olefinic H), 9.04 (s, 1H, CH of pyrazole); ^{13}C NMR (DMSO-d_6) δ (ppm): 26.34, 114.10, 116.34, 118.54, 119.13, 120.45, 125.32, 126.41, 129.31, 129.80, 129.94, 130.01, 132.40, 139.87, 149.31, 149.92, 151.27, 154.19;MS, m/z: 418 [$(M-1)^+$, 8.82%]; Anal. Calcd. For $C_{23}H_{17}N_9$ (419.16): C, 65.86; H, 4.09; N, 30.05, Found: C, 66.13; H, 4.13; N, 30.24.

4-((3-(4-(benzyloxy)phenyl)-1-phenyl-1*H*-pyrazol-4-yl)methylene)-5-imino-1-phenyl-4,5-dihydro-1*H*-pyrazol-3-amine **6a**

Yield 76%; m.p. 76-78 ºC; IR (KBr, cm^{-1}): 3281 (br., NH &

NH_2), 3031 (CH aromatic), 2932 (CH aliphatic), 1599 (C=N &C=C); ^{1}H NMR (DMSO-d_6) δ (ppm): 5.10 (s, 2H, OCH_2), 7.05 (d, 2H, aromatic H, *J* = 9 Hz), 7.33-7.68 (m, 15H, aromatic H), 7.93 (d, 2H, aromatic H, *J* = 9 Hz), 8.60 (s,1H, olefinic H), 8.93 (s, 1H, CH of pyrazole), 9.37 (s, 1H, NH; exchangeable with D_2O), 10.14 (s, 2H, NH_2; exchangeable with D_2O); ^{13}C NMR (DMSO-d_6) δ (ppm): 69.26, 114.86, 115.12, 117.47, 118.31, 124.96, 125.38, 126.42, 127.80, 128.72, 129.26, 129.45, 131.81, 136.91, 139.12, 150.44, 151.77, 156.61, 158.50;MS, m/z: 510 (M^+, 0.01%); Anal. Calcd. For $C_{32}H_{26}N_6O$ (510.22): C, 75.27; H, 5.13; N, 16.46, Found: C, 75.38; H, 5.20; N, 16.58.

2-((4-(4-(3-amino-5-imino-1-phenyl-1*H*-pyrazol-4(5*H*)-ylidene)methyl)-1-phenyl-1*H*-pyrazol-3-yl)phenyl)imino) methyl)malononitrile **6b**

Yield 70%; m.p. 157-159 °C; IR (KBr, cm^{-1}): 3340, 3223 (NH & NH_2), 3051 (CH aromatic), 2934 (CH aliphatic), 2191 (2 C≡N), 1623 (C=N), 1598 (C=C); ^{1}H NMR (DMSO-d_6) δ (ppm): 5.23 (s, 2H, NH_2; exchangeable with D_2O), 6.43 (d, 1H, $CH(CN)_2$, *J* = 8.4 Hz), 6.61 (d, 2H, aromatic H, *J* = 9 Hz), 6.68 (d, 1H, N=CH, *J* = 8.4 Hz), 6.73-7.93 (m, 12H, aromatic H), 8.68 (s,1H, olefinic H), 8.83 (s, 1H, CH of pyrazole), 10.08 (s, 1H, NH; exchangeable with D_2O);^{13}C NMR (DMSO-d_6) δ (ppm): 25.33, 112.18, 113.58, 114.07, 118.36, 118.86, 120.28, 125.99, 127.44, 128.76, 129.12, 129.30, 129.48, 129.92, 130.07, 130.36, 130.52, 149.49, 152.37, 154.28; MS, m/z: 496 [$(M+1)^+$, 0.36%]; Anal. Calcd. For $C_{29}H_{21}N_9$ (495.19): C, 70.29; H, 4.27; N, 25.44, Found: C, 70.48; H, 4.34; N, 25.53.

4.1.5. General procedure for the synthesis of compounds 7a,b

A mixture of compounds **4a,b** (0.001 mol), cyclohexanone (0.1 g, 0.001 mol) and ammonium acetate (0.08 g, 0.001 mol) in absolute ethanol (40 mL) was refluxed for 12h. The solid product was filtered off and crystallized from ethanol.

2-amino-4-(3-(4-(benzyloxy)phenyl)-1-phenyl-1*H*-pyrazol-4-yl)-5,6,7,8-tetrahydroquinoline-3-carbonitrile **7a**

Yield75%; m.p. 138-140 °C; IR (KBr, cm^{-1}): 3375 (NH_2), 3033 (CH aromatic), 2933 (CH aliphatic), 2209 (C≡N), 1605 (C=N), 1577 (C=C); ^{1}H NMR (DMSO-d_6) δ (ppm): 1.67-1.83 (m, 4H, cylohexane H), 2.56-2.70 (m, 4H, cyclohexane H), 5.17 (s, 2H, OCH_2), 6.57 (s, 2H, NH_2; exchangeable with D_2O), 7.00 (d, 2H, aromatic H, *J* = 9 Hz), 7.11-7.84 (m, 10H, aromatic H), 7.92 (d, 2H, aromatic H, *J* = 9 Hz), 8.72 (s, 1H, CH of pyrazole); ^{13}C NMR (DMSO-d_6) δ (ppm): 22.25, 24.94, 25.56, 69.24, 89.21, 113.92, 114.04, 114.86, 115.05, 115.56, 116.55, 118.07, 119.69, 124.93, 125.11, 126.35, 127.62, 128.49, 129.03, 129.18, 129.51, 136.82, 139.07, 139.19, 146.20, 148.83, 158.00, 158.34, 161.17;MS, m/z: 497 (M^+, 3.21%); Anal. Calcd. For $C_{32}H_{27}N_5O$ (497.22): C, 77.24; H, 5.47; N, 14.07, Found: C, 77.42; H, 5.53; N, 14.29.

2-(((4-(4-(2-amino-3-cyano-5,6,7,8-tetrahydroquinolin-4-yl)-1-phenyl-1*H*-pyrazol-3-yl)phenyl)imino)methyl) malononitrile **7b**

Yield 73%; m.p. 80-82 °C; IR (KBr, cm^{-1}): 3344, 3210 (NH_2), 3067 (CH aromatic), 2931 (CH aliphatic), 2215 (3 C≡N), 1608 (C=N &C=C); ^{1}H NMR (DMSO-d_6) δ (ppm): 1.50-1.55 (m, 2H, cyclohexane H), 1.65-1.70 (m, 2H, cyclohexane H), 2.21 (t, 2H, cyclohexane H), 2.76 (t, 2H, cyclohexane H), 4.15 (s, 2H, NH_2; exchangeable with D_2O), 7.34-7.73 (m, 7H, aromatic H), 7.89 (d, 2H, aromatic H, *J* = 9 Hz), 8.45 (s, 1H,CH-NH), 8.81 (s, 1H, CH of pyrazole), 11.17 (s, 1H, NH; exchangeable with D_2O); MS, m/z: 482 (M^+, 7.62%); Anal. Calcd. For $C_{29}H_{22}N_8$ (482.20): C, 72.18; H, 4.60; N, 23.22, Found: C, 72.35; H, 4.68; N, 23.41.

4.1.6. Synthesis of 5-(3-(4-(benzloxy)phenyl)-1-phenyl-1H-pyrazol-4-yl)-2H-1,2,4-triazol-3(4H)-one 8a

A mixture of compound **3** (0.35 g, 0.001 mol) and semicarbazide hydrochloride (0.11g, 0.001 mol) and crystalline sodium acetate (0.14g, 0.001 mol) in absolute ethanol (30 mL) was refluxed for 3h. After cooling and dilution with water, the product formed was filtered, washed with water, air dried and crystallized from absolute ethanol.

Yield 72%; m.p. 173-175 °C; IR (KBr, cm^{-1}): 3222, 3150 (2NH), 3042 (CH aromatic), 2916 (CH aliphatic), 1687 (C=O), 1599 (C=N &C=C); ^{1}H NMR (DMSO-d_6) δ (ppm): 5.18 (s, 2H, OCH_2), 6.39 (s, 1H, NH; exchangeable with D_2O), 7.12 (d, 2H, aromatic H, *J* = 9 Hz), 7.32-7.61 (m, 10H, aromatic H), 7.88 (d, 2H, aromatic H, *J* = 9 Hz), 9.02 (s, 1H, CH of pyrazole), 10.03 (s, 1H, NH; exchangeable with D_2O); ^{13}C NMR (DMSO-d_6) δ (ppm): 69.27, 114.90, 115.04, 117.47, 118.29, 124.96, 126.86, 127.73, 128.45, 129.31, 129.43, 131.72, 131.83, 136.91, 139.11, 150.44, 156.62, 158.49; MS, m/z: 410 [$(M+1)^+$, 1.79%]; Anal. Calcd. For $C_{24}H_{19}N_5O_2$ (409.15): C, 70.40; H, 4.68; N, 17.10, Found: C, 70.78; H, 4.75; N, 17.26.

4.1.7. Synthesis of 5-(3-(4-(benzloxy)phenyl)-1-phenyl-1H-pyrazol-4-yl)-2H-1,2,4-triazol-3(4H)-thione 8b

A mixture of compound **3** (0.35 g, 0.001 mol) and thiosemicarbazide (0.09 g, 0.001 mol) in absolute ethanol (30 mL) containing few drops of glacial acetic acid was refluxed for 3h. After cooling and dilution with water, the solid formed was filtered, washed with water, air dried and crystallized from absolute ethanol.

Yield 82%; m.p. 118-120 °C; IR (KBr, cm^{-1}): 3265, 3149 (2NH), 3030 (CH aromatic), 2926 (CH aliphatic), 1597 (C=N &C=C), 1176 (C=S); ^{1}H NMR (DMSO-d_6) δ (ppm): 4.47 (s,1H, NH; exchangeable with D_2O), 5.19 (s, 2H, OCH_2), 7.13 (d, 2H, aromatic H, *J* = 9 Hz), 7.34-7.73 (m, 10H, aromatic H), 7.87 (d, 2H, aromatic H, *J* = 9 Hz), 9.12 (s, 1H, CH of pyrazole), 11.27 (s, 1H, NH; exchangeable with D_2O); ^{13}C NMR (DMSO-d_6) δ (ppm): 69.77, 115.52,

117.42, 118.85, 125.32, 127.91, 128.14, 128.34, 128.93, 129.87, 130.10, 136.81, 137.40, 139.52, 151.60, 159.11, 179.10; MS, m/z: 425 (M^+, 0.37%); Anal. Calcd. For $C_{24}H_{19}N_5OS$ (425.13): C, 67.74; H, 4.50; N, 16.46, Found: C, 67.92; H, 4. 57; N, 16.63.

4.1.8. General procedure for the synthesis of compounds 9a,b

A mixture of compound **3** (0.34 g, 0.001 mol), ethyl cyanoacetate (0.11g, 0.001 mol) and urea or thiourea (0.001mol) in sodium ethoxide (0.5g of sodium in 20 ml ethanol) was stirred at room temperature for overnight. The reaction mixture was poured onto hydrochloric acid-ice. The solid formed was filtered off, washed with water, air dried and crystallized from ethanol.

6-(3-(4-(benzyloxy)phenyl)-1-phenyl-1*H*-pyrazol-4-yl)-2,4-dioxo-1,2,3,4-tetrahydropyrimidine-5-carbonitrile **9a**

Yield 58%; m.p. 135-137 ^oC; IR (KBr, cm^{-1}): 3347 (2NH), 3033 (CH aromatic), 2940 (CH aliphatic), 2221 (C≡N), 1692, 1637 (2 C=O), 1586 (C=N &C=C); ^1H NMR (DMSO-d_6) δ (ppm): 5.20 (s, 2H, OCH_2), 7.20 (d, 2H, aromatic H, *J* = 9 Hz), 7.35-7.83 (m, 10H, aromatic H), 7.91 (d, 2H, aromatic H, *J* = 9 Hz), 8.48 (s, 1H, NH; exchangeable with D_2O), 9.03 (s,1H, NH; exchangeable with D_2O), 9.15 (s, 1H, CH of pyrazole); ^{13}C NMR (DMSO-d_6) δ (ppm): 69.34, 101.42, 114.23, 115.20, 115.43, 116.60, 119.64, 123.14, 127.86, 128.54, 129.70, 130.13, 130.32, 136.77, 138.53, 144.84, 154.80, 159.24, 163.34; MS, m/z: 461 (M^+, 3.15%); Anal. Calcd. For $C_{27}H_{19}N_5O_3$ (461.15): C, 70.27; H, 4.15; N, 15.18, Found: C, 70.44; H, 4.19; N, 15.33.

6-(3-(4-(benzyloxy)phenyl)-1-phenyl-1*H*-pyrazol-4-yl)-4-oxo-2-thioxo-1,2,3,4-tetrahydropyrimidine-5-carbonitrile **9b**

Yield 69%; m.p. 108-110 ^oC; IR (KBr, cm^{-1}): 3190, 3128 (2NH), 3032 (CH aromatic), 2928 (CH aliphatic), 2215 (C≡N), 1677 (C=O), 1609 (C=N), 1598 (C=C), 1174 (C=S); ^1H NMR (DMSO-d_6) δ (ppm): 5.16 (s, 2H, OCH_2), 6.62 (s, 1H, NH; exchangeable with D_2O), 7.10 (d, 2H, aromatic H, *J* = 9 Hz), 7.34-7.84 (m, 12H, aromatic H), 8.53 (s, 1H, CH of pyrazole), 8.92 (s, 1H, NH; exchangeable with D_2O); MS, m/z: 477 (M^+, 1.13 %); Anal. Calcd. For $C_{27}H_{19}N_5O_2S$ (477.13): C, 67.91; H, 4.01; N, 14.67, Found: C, 68.08; H, 4.13; N, 14.88.

4.1.9. General procedure for the synthesis of compounds 10a,b and 11a,b

A mixture of compound **3** (0.35 g, 0.001 mol), urea or thiourea (0.001 mol) and acetyl acetone or ethylacetoacetate (0.001 mol) in absolute ethanol (20 mL) containing few drops of hydrochloric acid was refluxed for 4-6h. After cooling, the solid formed was filtered off, washed with water, air dried and crystallized from ethanol.

5-acetyl-4-(3-(4-benzyloxy)phenyl)-1-phenyl-1*H*-pyrazol-4-yl)-6-methylpyrimidin-2(1*H*)-one **10a**

Yield 67%; m.p. 165-167 ^oC; IR (KBr, cm^{-1}): 3174 (NH), 3032 (CH aromatic), 2929 (CH aliphatic), 1704, 1651 (2C=O),1601 (C=N &C=C); ^1H NMR (DMSO-d_6) δ (ppm): 1.24 (s, 3H, CH_3), 2.43 (s, 3H, $COCH_3$), 5.20 (s, 2H, OCH_2), 7.19 (d, 2H, aromatic H, *J* = 9 Hz), 7.35-7.69 (m, 10H, aromatic H), 7.94 (d, 2H, aromatic H, *J* = 9 Hz), 9.26 (s, 1H, CH of pyrazole); ^{13}C NMR (DMSO-d_6) δ (ppm): 19.4, 56.4, 69.71, 110.00, 115.68, 119.13, 124.30, 126.43, 127.82, 128.17, 128.95, 129.54, 130.45, 137.33, 150.41, 156.52, 159.21, 193.10; MS, m/z: 476 (M^+, 2.68 %); Anal. Calcd. For $C_{29}H_{24}N_4O_3$ (476.18): C, 73.09; H, 5.08; N, 11.76, Found: C, 73.05; H, 5. 59; N, 11.88.

5-acetyl-4-(3-(4-benzyloxy)phenyl)-1-phenyl-1*H*-pyrazol-4-yl)-6-methylpyrimidin-2(1*H*)-thione **10b**

Yield 62%; m.p. 200-202 ^oC; IR (KBr, cm^{-1}): 3296 (NH), 3055 (CH aromatic), 2957 (CH aliphatic), 1706 (C=O), 1619 (C=N), 1594 (C=C) 1180 (C=S); ^1H NMR (DMSO-d_6) δ (ppm): 1.90 (s, 3H, CH_3), 2.43 (s, 3H, $COCH_3$), 5.20 (s, 2H, OCH_2), 7.19-8.22 (m, 14H, aromatic H), 9.43 (s, 1H, CH of pyrazole), 10.47 (s, 1H, NH; exchangeable with D_2O); ^{13}C NMR (DMSO-d_6) δ (ppm): 21.3, 30.08, 69.30, 111.20, 115.09, 118.33, 124.59, 127.77, 128.40, 129.54, 136.87, 139.01, 143.78, 158.28, 163.21, 173.76, 203.87; MS, m/z: 492 (M^+, 3.44 %); Anal. Calcd. For $C_{29}H_{24}N_4O_2S$ (492.16): C, 70.71; H, 4.91; N, 11.37, Found: C, 70.58; H, 5. 37; N, 11.47.

Ethyl 4-(3-(4-(benzyloxy)phenyl)-1-phenyl-1*H*-pyrazol-4-yl)-6-methyl-2-oxo-1,2,3,4-tetrahydropyrimidine-5-carboxylate **11a**

Yield 81%; m.p. 98-100 ^oC; IR (KBr, cm^{-1}): 3341, 3145 (2NH), 3032 (CH aromatic), 2919 (CH aliphatic), 1701, 1655 (2C=O), 1596 (C=N &C=C); ^1H NMR (DMSO-d_6) δ (ppm): 1.04 (t, 3H, CH_2-$\underline{CH_3}$), 2.27 (s, 3H, CH_3), 3.42 (q, 2H, $\underline{CH_2}$-CH_3), 5.18 (s, 2H, OCH_2), 5.38 (s, 1 H, CH of pyrimidine), 6.95-8.43 (m, 14H, aromatic H), 9.17 (s, 1H, CH of pyrazole), 9.30 (s, 1H, NH; exchangeable with D_2O), 9.98 (s, 1H, NH; exchangeable with D_2O); ^{13}C NMR (DMSO-d_6) δ (ppm): 14.20, 18.14, 59.89, 69.72, 105.37, 115.49, 118.54, 126.02, 127.25, 128.09, 128.29, 128.88, 129.62, 129.94, 137.46, 140.12, 152.18, 158.79, 166.12; MS, m/z: 508 (M^+, 1.08%); Anal. Calcd. For $C_{30}H_{28}N_4O_4$ (508.21): C, 70.85; H, 5.55; N, 11.02, Found: C, 70.97; H, 5. 61; N, 11.18.

Ethyl 4-(3-(4-(benzyloxy)phenyl)-1-phenyl-1*H*-pyrazol-4-yl)-6-methyl-2-thioxo-1,2,3,4-tetrahydropyrimidine-5-carboxylate **11b**

Yield 64%; m.p. 145-147 ^oC; IR (KBr, cm^{-1}): 3335, 3170 (2NH), 3032 (CH aromatic), 2929 (CH aliphatic), 1709 (C=O), 1602 (C=N), 1579 (C=C) 1175 (C=S); ^1H NMR (DMSO-d_6) δ (ppm): 0.82 (t, 3H, CH_2-$\underline{CH_3}$), 1.90 (s, 3H,CH_3), 3.80 (q, 2H, $\underline{CH_2}$-CH_3), 5.18 (s, 2H, OCH_2), 5.36 (s, 1H, CH of pyrimidine), 7.07 (d, 2H, aromatic H, *J* =9 Hz), 7.11-7.96 (m, 12H, aromatic H), 9.29 (s, 1H, CH of

pyrazole), 9.67 (s, 1H, NH; exchangeable with D_2O), 10.24 (s, 1H, NH; exchangeable with D_2O); MS, m/z: 524 (M^+, 1.01%); Anal. Calcd. For $C_{30}H_{28}N_4O_3S$ (524.19): C, 68.68; H, 5.38; N, 10.68, Found: C, 68.89; H, 5. 46; N, 10.89.

4.2. In vitro anti-tumor assay

4.2.1. Methodology: cell culture

Cancer cells from breast cancer cell line (MCF7, human breast adenocarcinoma) was purchased from American type Cell Culture collection (ATCC, Manassas, USA) and grown on the appropriate growth medium Dulbecco's modified Eagle's medium (DMEM) or Roswell Park Memorial Institute medium (RPMI 1640) supplemented with 100 mg/ mL of streptomycin, 100 units/ mL of penicillin and 10% of heat-inactivated fetal bovine serum in a humidified, 5% (v/v) CO_2 atmosphere at 37 ºC

4.2.2. Cell growth inhibitory assay

Cytotoxicity was determined using 3-[4,5-dimethylthiazole-2-yl]-2,5-diphenyltetrazolium bromide (MTT) method. Exponentially growing cells were trypsinized, counted and seeded at the appropriate densities (2000-1000 cells/0.33 cm^2 well) into 96-well microtiter plates. Cells then were incubated in a humidified atmosphere at 37˚C for 24 hours. Then, cells were exposed to different concentrations of compounds (0.1, 10, 100, 1000 µM) for 72 h. Then the viability of treated cells was determined using MTT technique as follow. Media were removed; cells were incubated with 200 µl of 5% MTT solution/well (Sigma Aldrich, MO) and were allowed to metabolize the dye into colored-insoluble formazan crystals for 2 h. The remaining MTT solution were discarded from the wells and the formazan crystals were dissolved in 200 µl/well acidified isopropanol for 30 min, covered with aluminum foil and with continuous shaking using a MaxQ 2000 plate shaker (Thermo Fisher Scientific Inc, MI) at room temperature. Absorbances were measured at 570 nm using a Stat FaxR 4200 plate reader (Awareness Technology, Inc., FL). The cell viability were expressed as percentage of control and the concentration that induces 50% of maximum inhibition of cell proliferation (IC50) were determined using Graph Pad Prism version 5 software (Graph Pad software Inc, CA) [29,30].

4.2.3. Immune-fluorescence staining

Cells were cultured on sterile cover slips (22 mm^2, Harvard Apparatus) in sterile six well plates at a density of 2×10^5 cells/well. After 24 h, cells were exposed to the pre-determined IC_{50} of the test compound in fresh medium for 24 h. At the end of the exposure, cells attached to cover slips were washed with PBS and fixed with 3.7% paraformaldhyde for 10 min and permeabilized with 0.25% Triton X-100 in TBST containing 0.01% Tween 20 for 10 min. 4',6'-Diamidino-2-Phenylindole, dihydrochloride (DAPI) (Sigma-Aldrich, St. Louis, MO, USA) was used as nuclear stain. The cover slips with cells were then mounted on a glass slide with anti-fade mounting medium and viewed with an epifluorescence microscope, Leica, DM 5500 B (Leica, Buffalo Grove, IL, USA) at a magnification of 60×.

4.2.4. Cell Cycle Analysis (DNA-Flow Cytometry Analysis):

MCF7 cells at a density of 4 x106 cells by T 75 flask were exposed to (Compound X) at its IC_{50} for 24 h. The cells then were collected by trypsinization, washed in phosphate buffered saline and fixed in ice-cold absolute alcohol. Thereafter, cells were stained using Cycle TEST™ PLUS DNA Reagent Kit (BD Biosciences, San Jose, CA) according to the manufacturer's instructions. Cell-cycle distribution was determined using a FACS Calibur flow cytometer (BD Biosciences, San Jose, CA).

References

[1] M. Vosooghi, L. Firoozpour, A. Rodaki, M. Pordeli, M. Safavi, S. K. Ardestani, A. Dadgar, A. Asadipour, M. H. Moshafi, A. Foroumadi, *DARU J. Pharm. Sci.* 22 (2014) 83-89.

[2] A. K. El-Ansary, A. M. Kamal, M. A. Al-Ghorafi, *Eur. J. Med. Chem.* 86 (2014) 202-210.

[3] A. Kumar, G. Gupta, A. K. Bishnoi, R. Saxena, K. S. Saini, R. Konwar, S. Kumar, A.Dwivedi, *Bioorg. Med. Chem.* 23 (2015) 839-848.

[4] V. R. Solomon, H. Lee, *Biomed. Pharmacother.* 66 (2012) 213–220.

[5] N. Inceler, A. Yılmaz, S. N. Baytas, *Med. Chem. Res*. 22 (2013) 3109–3118.

[6] J. Bronson, M. Dhar, W. Ewing, N. Lonberg, *Annu. Rep. Med. Chem*. 47 (2012) 548.

[7] J. Bronson, M. Dhar, W. Ewing, N. Lonberg, *Annu. Rep. Med. Chem*. 47 (2012) 525.

[8] S. N. Baytas, N. Inceler, A. Yılmaz, *Med. Chem. Res*. 22 (2013) 4893–4908.

[9] R. K. Yadlapalli, O.P. Chourasia, K. Vemuri, M. Sritharan, R. S. Perali, *Bioorg. Med. Chem. Lett.* 22 (2012) 2708-2711.

[10] S. A. F. Rostom, *Bioorg. Med. Chem.* 18 (2010) 2767-2776.

[11] A. H. Abadi, A. A. H. Eissa, G. S. Hassan, *Chem. Pharm. Bull*. 51 (2003) 838-844.

[12] X. Huang, X. Lu, Y. Zhang, G. Song, Q. He, Q. Li, X. Yang, Y. Wei, H. Zhu, *Bioorg. Med. Chem*., 20 (2012) 4895−4900.

[13] M. F. Mohamed, M. S. Mohamed, M. M. Fathi, S. A. Shouman, I. A. Abdelhamid, *Anticancer Agents Med. Chem.* 14 (2014) 1282-1292.

[14] F. A. Ragab, N. M. Abdelgawad, H. H. Georgey, M. F. Said, *Eur. J. Med. Chem.* 63 (2013) 645-654.

[15] A. H. F. Abd El-Wahab, Z. I. A. Al-Fifi, A. H. Bedair, F. M. Ali, A. H. A. Halawa, A. M. El-Agrody, *Molecules* 16 (2011) 307-318.

[16] N. I. Abdel Sayed, *Egypt. J. Chem*. 51 (1999) 175-187.

[17] Y. M. Elkholy, M. A. Morsy, *Molecules* 11 (2006) 890-903.

[18] H. H. Fahmy, N. M. Khalifa, E. S. Nossier, M. M. Abdalla, M. M. F. Ismail, *ActaPol. Pharm*. 69 (2012) 411-421.

[19] O. A. Fathalla, I. F. Zeid, M. E. Haiba, A. M. Soliman, Sh. I. Abd-Elmoez , W. S. El-Serwy, World Journal of Chemistry 4 (2009) 127-132.

[20] M. I. El-zahar, S. S. Abd El Karim, M. E. Haaiba, M. A. Khedr, *ActaPol. Pharm*. 68 (2011)

357-373.

[21] D. Barnum, J. Greene, A. Smellie, P. Sprague, *J. Chem. Inf. Comput. Sci*. 36 (1996) 563-

571.

[22] A. Smellie, S.L. Teig, P. Towbin, *J. Comput. Chem*. 16 (1995) 171-187.

[23] M.O. Taha, Y. Bustanji, M.A.S. Al-Ghussein, M. Mohammad, H. Zalloum, I.M. Al- Masri, N. Atallah, *J. Med. Chem*. 51 (2008) 2062-2077.

[24] M.O. Taha, Y. Bustanji, A.G. Al-Bakri, A. Yousef, W.A. Zalloum, I.M. Al-Masri, N. Atallah, *J. Mol. Graph. Model*. 25 (2007) 870-884.

[25] R. Abu Khalaf, G. Abu Sheikha, Y. Bustanji, M.O. Taha, *Eur. J. Med. Chem*. 45 (2010)1598-1617.

[26] A. S. Girgis, J. Stawinski, N. S. M. Ismail, H. Farag, *Eur. J. Med. Chem*. 47 (2012) 312-322.

[27] X. Alejandro, Dominguez, B. Gomez, E. Homberag, J. Slim, *J. Amer. Chem. Soc*. 77 (1955) 1288-1290.

[28] A. M. Asiri, A. A. Bahajaj, I. M. I. Ismail, N. A. Fatani, *Dyes Pigm.*, 71 (2006), 103-108.

[29] T. Mosmann, *J Immunol Methods* 65 (1983) 55-63.

[30] D. A. Scudiero, D. A. Scudiero, R. H. Shoemaker, K. D. Paull, A. Monks, S. Tierney, T. H. Nofziger, M. J. Currens, D. Seniff, M. R. Boyd, *Cancer Res*. 48 (1988) 4827-4833.